Tellus (1998), 50B, 93–109
Printed in UK – all rights reserved

TELLUS
ISSN 0280–6509

A note on the C/N and C/P ratio of the biological production in the Nordic seas

By GÖRAN BROSTRÖM *Göteborg University, Department of Oceanography, Box 460, S-405 30 Gothenburg, Sweden*

(Manuscript received 4 June 1996; in final form 8 October 1997)

ABSTRACT

In this paper, we study the consumption of carbon, nitrogen and phosphate in the upper layer of the Nordic seas. It is found that the biological draw-down of nutrient concentrations and dissolved inorganic carbonate concentration, C_T, during summer cannot be explained in terms of the common Redfield ratio (C : N : P = 106 : 16 : 1) for organic material. According to Børsheim and Myklestad, the seasonal variation of dissolved organic carbon, DOC, concentration is of order 20 μmol/kg. Based on these measurements, we argue that production of DOC with a high carbon content (C : N ≈ 15) is the main cause of the high consumption of C_T. Further, there are indications that we need a C : N = 9 ratio for organic material to complete the upper ocean carbon budget at station M. However, the uncertainty in the gas exchange formulation, which is of order 30%, makes this kind of interpretation of data vulnerable. The flux of CO_2 from the atmosphere happens to cancel the influence of DOC on the C_T. Thus, an interpretation of data, without considering the air-sea gas exchange, will falsely reveal that the production follows the Redfield ratio.

1. Introduction

New measuring techniques for chemical variables have lead to new results about the oceanic carbon cycle. Simultaneous measurements of total dissolved inorganic carbonate concentration, C_T, and nitrate concentration, NO_3, reveal that the draw-down of C_T relative NO_3 during periods of biological production does not follow the Redfield ratio (Codispoti et al., 1982, 1986; Sambrotto et al., 1993; Sambrotto and Langdon, 1994; Michaels et al., 1994; Bates et al., 1996; Marchal et al., 1996).

Sambrotto et al. (1993) concluded that the Redfield ratio (in this work used for a C : N : P = 106 : 16 : 1 ratio) may underestimate the C_T draw-down by a factor 2 during the North Atlantic spring bloom. Sambrotto and Langdon (1994) studied the water column budget of the George Bank spring bloom and attributed the large removal of C_T to production of organic material rich in carbon. Chen et al. (1996) showed that the dissolved organic carbon, DOC, concentration has a strong vertical gradient at the George Bank spring bloom. Production of DOC (without the corresponding production of dissolved organic nitrogen) may enhance the draw-down of C_T explaining part of the carbon budget at George Bank.

An extreme example of the imbalance in the upper ocean carbon cycle is found at the Bermuda Atlantic Time Serie (BATS). Although the position of the time serie was chosen at a previously well studied position (Mentzel and Ryther, 1960) there is a significant decrease in C_T during the summer months that, presently, cannot be accounted for (Michaels et al., 1994; Toggweiler, 1994; Bates et al., 1996; Marchal et al., 1996). There have been

E-mail: gobr@oce.gu.se

speculations that advection of water with low C_T may be a part of the explanation (Toggweiler, 1994; Follows et al., 1996). However, recent results indicate that the summer decrease in C_T probably is the result of biological processes (Bates et al., 1996). Although the production of DOC cannot explain the carbon imbalance at BATS it is dynamically very important as it may dominate the flux of carbon from the euphotic zone to the winter mixed layer (Carlson et al., 1994; Guo et al., 1995).

Takahashi et al. (1985) suggested, from observations along isopycnal surfaces in the deep water, that the C : N ratio of organic material that degenerates in the deep water is between 103 : 16 and 140 : 16. The lower value was estimated from C_T measurements and the upper value was based on the oxygen utilization. However, the oxygen content of organic material may still involve some uncertainties (Anderson & Sarmiento, 1994; Anderson, 1995) and the latter number may be unsure. Nevertheless, Takahashi et al. suggested that $P:N:C = 1:16:122(\pm 18)$ for the Atlantic and Indian Oceans.

In this work we intend to study the signature of the biological cycle in the Nordic seas. For a precise interpretation of C_T data we need a full history of the gas flux through the sea surface, mixed layer depth, mixing with deeper waters, lateral advection and a history of the biological production (Codispoti et al., 1982, 1986; Takahashi et al., 1985, 1993; Peng et al., 1987). We do not have the data necessary to perform such calculations and we will compare available data with some results from a physical-biological-chemical model described in Section 2. By that we may find how different assumption on the carbon dynamics compares with data.

Data we use in this study are NO_3, C_T and DOC concentrations at station M (66°N, 2°E) (F. Rey, personal communication; Gislefoss, 1994; Børsheim and Myklestad, 1997), we also consider some stations from the TTO/NAS expedition and measurements from the Mosby cruise in 1991 (Brewer et al., 1986; Lundberg et al., 1995). The positions of the stations are shown in Fig. 1. Station 158 in the TTO/NAS expedition has not been used as its surface values of C_T and total alkalinity concentration are much lower than the surrounding stations.

In Section 2 we will describe the model including a section for the physical model, a section for the biological model, a section for the DOC dynamics and, finally, a section for the chemical model. Some results from the model are presented in Section 3 where we also compare model results with measurements. Finally, we end with a discussion of the results in Section 4.

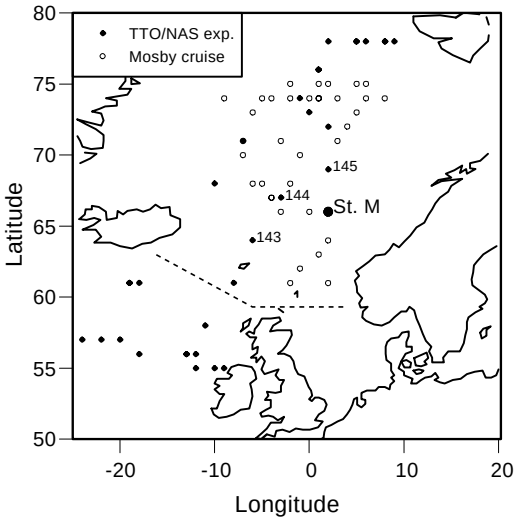

Fig. 1. A map showing the position of station M, the TTO/NAS stations and the Mosby 1991 cruise stations that have been used in this study. The TTO/NAS expedition was in the Norwegian sea between 25 July and 6 August 1981. The Mosby cruise was in the Norwegian sea from 14 August through 8 September 1991. Stations 143–145 from the TTO/NAS expedition are numbered in the figure. The dashed lines show the stations that are included in this study.

2. The model

2.1. *Short summary of the model*

The model is built from a one-dimensional k-ε turbulence model (Rodi, 1980, 1987) that is forced by meteorological observations taken at station M. To fit observations of temperature we have modified the turbulence scheme to include mixing in the thermocline (Gargett, 1984) and added an internal heat source interpreted as large scale advection of heat.

The biological model contains 4 variables, namely, nutrient and phytoplankton concentrations, the total amount of zooplankton in the

upper water column and the detritus concentration. At station M there is only a minor phytoplankton spring bloom, possibly, it is zooplankton grazing that limits the phytoplankton bloom (Bathmann et al., 1990). Østvedt (1955) showed that the major copepods (i.e., *Calanus finmarchius* and *Pseudocalanus*) at station M may overwinter in the deep water and we describe the exchange of zooplankton between deep water and the upper layer.

One of the aims with this study is to investigate the role of DOC in the upper ocean carbon budget. Thus, we need to describe the DOC dynamics and the features of the microbial loop (Taylor and Joint, 1990). We rely on a simple model that only contains the labile DOC concentration and the model is easy to tune to data. The model is, however, based on the properties of the microbial loop which basic features are described in Appendix A.

The chemical variables that we consider are C_T, and the total alkalinity concentration, A_T, which both are normalized to 35 psu. C_T is coupled to the biological model by a material dependent C : N ratios. The production/destruction of DOC is also important for the C_T. We neglect all effects from Calciumcarbonates producing organisms (Peng et al., 1987) an assumption that is verified by measurements from the TTO/NAS and Mosby expeditions. Accordingly variations in A_T are fully determined by variations in the dissolved nitrate concentration.

2.2. Physical model

2.2.1. Basic equations. We consider a one-dimensional model where the turbulent mixing is described according to the eddy viscosity concept (Rodi, 1980, 1987). The conservation equations for momentum, heat and salt become,

$$\frac{\partial u}{\partial t} - fv = \frac{\partial}{\partial z}\left[v_t \frac{\partial u}{\partial z}\right],$$

$$\frac{\partial v}{\partial t} + fu = \frac{\partial}{\partial z}\left[v_t \frac{\partial v}{\partial z}\right],$$

$$\frac{\partial T}{\partial t} = \frac{\partial}{\partial z}\left[v_t \frac{\partial T}{\partial z}\right] + \frac{1}{c_p \rho}\frac{\partial I}{\partial z} + Q_{in},$$

$$\frac{\partial S}{\partial t} = \frac{\partial}{\partial z}\left[v_t \frac{\partial S}{\partial z}\right], \qquad (1a–d)$$

where u and v are the velocity components in the x and y directions, respectively, v_t is the eddy viscosity (the same for all variables except for the turbulent kinetic energy, k, and its dissipation rate, ε), f is the Coriolis parameter, T and S are temperature and salinity, I is the solar radiation, ρ is the density of water, c_p is the specific heat of water and Q_{in} is an internal heat source interpreted as large scale advection in combination with a temperature gradient.

2.2.2. Boundary and initial conditions. The boundary conditions to eqs. (1) are:

$$v_t\left[\frac{\partial u}{\partial z}, \frac{\partial v}{\partial z}, \frac{\partial T}{\partial z}, \frac{\partial S}{\partial z}\right] = \left[\frac{\tau_x}{\rho}, \frac{\tau_y}{\rho}, \frac{Q}{c_p \rho}, S(E-P)\right] \quad \text{at } z=0, \qquad (2a–d)$$

$$v_t\left[\frac{\partial u}{\partial z}, \frac{\partial v}{\partial z}, \frac{\partial T}{\partial z}, \frac{\partial S}{\partial z}\right] = 0 \quad \text{at } z=-H, \qquad (2e–h)$$

where -H is the bottom of the model domain. (τ_x, τ_y) is the wind stress vector, Q is the heat flux at the sea surface and $E-P$ is the net evaporation. Large and Pond (1981) presented a relation between wind at 10 m height and the stress at the sea surface and we use this. Q is calculated from air temperature, sea surface temperature, wind speed and humidity using the formulas presented by Häkkinen and Cavalieri (1989). $E-P$ is given as:

$$E-P = A\cos(\omega t),$$

where $A = -0.35 \cdot 2\pi$ m/year and $\omega = 2\pi$ year^{-1}. The formula is based on the fresh water content in the upper 100 m during the summer months.

The initial conditions for temperature and salinity are: $T = 8°C$ in the upper 200 m, then decreasing linearly to 0°C at 500 m, $S = 35.2$ psu in the upper 200 m, then decreasing linearly to 35 psu at 500 m.

2.2.3. Solar radiation. Häkkinen and Cavalieri (1989) described a formula for the solar radiation given as,

$$Q_{sw\text{-}direct} = (1-a)a^* Q_0, \qquad (3a)$$

where $Q_{sw\text{-}direct}$ is the direct incoming solar radiation and $a = 0.1$ is the albedo. To complete the upper ocean heat budget for station M we prescribe that 25% of the scattered light reaches

the sea surface,

$$Q_{\text{sw-scatter}}=(1-a)(1-a^*)0.25Q_0, \tag{3b}$$

where $Q_{\text{sw-scatter}}$ is the light that reaches the sea surface as diffusive light. In the above formulas we have the following quantities: $a^*=1-0.6C^3$ is cloud correction where C is the fraction of cloud cover; $Q_0=S_0\cos^2 z/(1.085\cos z+(2.7+\cos z)e_a\cdot 10^{-3}+0.1)$ where $S_0=1353$ W/m^2 is the solar constant and e_a is the water vapor pressure at 10 m; z is the sun zenith angle given by $\cos z=\sin\phi\sin\delta+\cos\phi\cos\delta\cos HA$ where ϕ is the latitude, $\delta=23.44^\circ\cos[(172\text{-day of year})\pi/180]$ and $HA=12$-*local time* is the local solar time. Further, we assume that 50% of the solar radiation is long wave radiation that is captured in the uppermost cms of the ocean.

The remaining 50% is considered as photosynthetically active radiation and it is distributed in the ocean as,

$$\frac{\partial I}{\partial z}=(k_0+k_P P)I/G, \tag{4}$$

where k_0 is the extinction coefficient for pure sea water and k_P is a constant such that $k_P P$ is the extinction coefficient caused by the phytoplankton. G is a geometrical factor given by (Sathyendranath and Platt, 1988),

$$G=\begin{cases}\sqrt{1-(\cos(\lambda)/1.33)^2} & \text{direct light,}\\ 0.87 & \text{diffusive light,}\end{cases} \tag{5}$$

where λ is the solar altitude and is given from $\sin\lambda=\cos z$.

2.2.4. Turbulence model. The turbulent exchange coefficient is calculated according to the $k-\varepsilon$ model (Rodi, 1980, 1987). Variables in the $k-\varepsilon$ model are the turbulent kinetic energy, k, and its dissipation rate, ε, and v_t is related to these. The model equations are,

$$\frac{\partial k}{\partial t}=\frac{\partial}{\partial z}\left[\frac{v_t}{\sigma_k}\frac{\partial k}{\partial z}\right]+P_S+P_B-\varepsilon,$$

$$\frac{\partial \varepsilon}{\partial t}=\frac{\partial}{\partial z}\left[\frac{v_t}{\sigma_\varepsilon}\frac{\partial \varepsilon}{\partial z}\right]+\frac{\varepsilon}{k}(C_{1\varepsilon}P_S+C_{3\varepsilon}P_B-C_{2\varepsilon}\varepsilon),$$

$$v_t=C_\mu\frac{k^2}{\varepsilon}, \tag{6a–c}$$

where,

$$P_S=v_t\left[\left(\frac{\partial u}{\partial z}\right)^2+\left(\frac{\partial v}{\partial z}\right)^2\right],$$

$$P_B=v_t g\left[-\alpha\frac{\partial T}{\partial z}+\beta\frac{\partial S}{\partial z}\right]. \tag{6d, e}$$

C_μ, $C_{1\varepsilon}$, $C_{2\varepsilon}$, $C_{3\varepsilon}$, σ_k and σ_ε are empirical constants in the model, g is gravity, P_S is the production of turbulence due to shear, P_B is the production or destruction due to buoyancy effects. Finally, α and β are constants in the linearized equation for density,

$$\rho(T,S)=\rho_0(1-\alpha(T-T_0)+\beta(S-S_0)), \tag{7}$$

where ρ_0, T_0 and S_0 are reference density, temperature and salinity, respectively.

With a stable stratification, the k-ε model requires a velocity shear to produce mixing, the model formulation implies that only small amounts of the momentum slip through the bottom of the mixed layer. Therefore, the model produces very weak mixing in, e.g., the thermocline. The mixing in these regions may be forced by internal waves etc. that are not described in the k-ε model and we need an alternative turbulence scheme to describe the mixing. Gargett (1984) proposed that mixing below the bottom of the mixed layer can be described as:

$$v_t=\frac{a_0}{N}, \tag{8a}$$

where,

$$N^2=-\frac{g}{\rho}\frac{\partial \rho}{\partial z}, \tag{8b}$$

and a_0 is a constant. Gargett suggested that $a_0=1\cdot 10^{-7}$ m^2/s^2, however, with this value the mixing in the thermocline is too small to reproduce data and we use $a_0=4\cdot 10^{-7}$ m^2/s^2.

We have two formulations of the turbulent exchange coefficient, the k-ε model and the Gargett (1984) formulation. We can only use one description at each depth and use whichever model that produces the largest mixing.

With boundary conditions for k and ε (Rodi, 1980), eqs. (1)–(8) form a closed set of equations. The equations are solved with the numerical method implemented in the PROBE routine, developed at SMHI (Swedish Meteorological and Hydrological Institute; Svensson, 1986). PROBE

Table 1. *Numerical values of constants involved in the physical model*

Constant	Meaning	Value
C_μ	constant in turbulence model	0.09
$C_{1\varepsilon}$	constant in turbulence model	1.44
$C_{2\varepsilon}$	constant in turbulence model	1.92
$C_{3\varepsilon}$	constant in turbulence model	0.8
σ_k	Prandtl/Schmidt number for k	1.4
σ_ε	Prandtl/Schmidt number for ε	1.3
a_0	strength of thermocline mixing	$4\cdot10^{-7}$ m^2 s^{-2}
ρ_0	reference density	1027 kgm^{-3}
T_0	reference temperature	10°C
S_0	reference salinity	35 psu
α	temperature expansion coefficient	$1.5\cdot10^{-4}$°C^{-1}
β	salinity expansion coefficient	$8\cdot10^{-4}$ psu^{-1}
f	Coriolis parameter	$1.32\cdot10^{-4}$ s^{-1}
c_P	heat capacity of water	$4.18\cdot10^3$ J/kg
k_0	light extinction coefficient for pure water	0.05 m^{-1}
k_P	Parameter in light extinction coefficient	0.05 (μmol/kg m)$^{-1}$

uses a finite difference scheme based on an implicit code. Maximum depth is 500 m and we use 200 grid points. The grid is non-uniform and has 1 meter resolution at the sea surface and about 15 m at the bottom. To integrate the model forward in time we use 300 s time steps. Numerical values of the constants in the physical model are presented in Table 1.

2.3. *Biological model*

The 4 variables in the biological model are the concentrations of nutrient, N, and phytoplankton, P, the total amount of zooplankton, Z_{tot}, and detritus concentration, D. Nitrate and ammonia may easily be distinguished in the model, however, that will add complexity to the model without adding any further information of the carbon system.

2.3.1. The mathematical formulation. The mathematical formulation of the biological model are given as,

$$\mathscr{F}(N) = -G_P + M_P + M_Z + M_D + F,$$

$$\mathscr{F}(P) = \frac{\partial w_P P}{\partial z} + G_P - M_P - G_Z,$$

$$\frac{dZ_{\text{tot}}}{dt} = \int_{-\infty}^{0} (G_Z - E_Z - M_Z)\, dz + S,$$

$$\mathscr{F}(D) = \frac{\partial w_D D}{\partial z} + E_Z - M_D, \qquad (9a–d)$$

where,

$$\mathscr{F} = \frac{\partial}{\partial t} - \frac{\partial}{\partial z}\left[v_t \frac{\partial}{\partial z} \right].$$

The variables N, P, Z_{tot} and D are measures of the nitrogen content in the different states. Furthermore, G_P is the growth of phytoplankton, M_P is the metabolism for phytoplankton, M_Z is the metabolism for zooplankton, M_D is the bacterial metabolism of detritus, G_Z is the growth of zooplankton, E_Z is the zooplankton egestion rate, S describes movements of zooplankton between deeper layers and the upper ocean, finally, w_P and w_D are the sinking velocities for phytoplankton and detritus, respectively.

F is the flux of nutrient according to the DOC model and will be described in Subsection 2.4.

The fluxes between the variables in the biological model are given by:

$$G_P = \gamma_P g(T) I_{\lim}(I) \left(\frac{N}{\kappa_N + N} \right) P,$$

$$M_P = \mu_P g(T) P,$$

$$G_Z = \gamma_Z g(T) \left(\frac{P^2}{\kappa_P^2 + P^2} \right) Z,$$

$$E_Z = \varepsilon_Z G_Z,$$

$$M_Z = g(T)({}^1\mu_Z + {}^2\mu_Z Z) Z,$$

$$M_D = \mu_D D, \qquad (10a–f)$$

where,

$$g(T)=e^{b(T-10)},$$

$$I_{\lim}(I)=1-e^{I/\kappa_I},$$

$$Z=\frac{P}{\int_{-\infty}^{0} P\,dz}\,Z_{\text{tot}}, \qquad (10g\text{–}i)$$

where the constants are described in subsections 2.3.3–2.3.5. Eq. (10i) describes how the zooplankton biomass is distributed. The assumption is that zooplankton distribute themselves instantaneously according to the phytoplankton concentration.

The flux of zooplankton between deep waters and the surface layer is described as:

$$S=\begin{cases} S^{\text{u}} & 100<t<130 \\ -S^{\text{d}} & 210<t<240 \\ 0 & \text{otherwise,} \end{cases} \qquad (11)$$

where S^{u} denotes the upward motion and S^{d} the downward motion.

Bathmann et al. (1990) reported, for February 1987, a deep water zooplankton population of 1.5 gC/m^2, if we assume that all these zooplankton move to the surface in 30 days we have that $S^{\text{u}}=$ 0.67 μmol m/(kg day). It may be interesting to consider an equation for the deep dwelling zooplankton, however, since we run the model for one year we see no point in considering this complication of the model. To account for the loss of zooplankton in the winter deep water, we prescribe somewhat arbitrarily $S^{\text{d}}=3S^{\text{u}}$.

The numerical values of constants in the biological model are described in Table 2.

2.3.2. Boundary and initial conditions. As boundary conditions for the biological components we apply zero flux conditions,

$$\left\{v_t\left(\frac{\partial N}{\partial z},\frac{\partial P}{\partial z},\frac{\partial D}{\partial z}\right)+(0,\,w_{\text{P}}P,\,w_{\text{D}}D)\right\} = \begin{cases} 0 & \text{at } z=0, \\ 0 & \text{at } z=-H. \end{cases} \qquad (12a\text{–}c)$$

This condition implies an accumulation of nutrients in the bottom water. However, as $-H$ is well below the winter mixed layer depth the accumulation of nutrients in the lowest part of the grid will only have negligible influence on the modeled annual cycle.

As initial conditions we prescribe,

$$(N,\,P,\,D)=(12,\,0.03,\,0)\ \mu\text{mol/kg}, \qquad (13a\text{–}c)$$

$$Z_{\text{tot}}=10\ \mu\text{mol m/kg}. \qquad (13d)$$

2.3.3. Details of phytoplankton equation. The growth of phytoplankton, G_{P}, involves a rate constant, γ_{P}, a temperature dependence, $g(T)$, governed by the parameter b, the light intensity

Table 2. *Numerical values of constants involved in the biological model*

Constant	Meaning	Value
γ_{P}	phytoplankton growth rate	1.1 day^{-1}
b	phytoplankton growth, temperature dependence	0.06°C^{-1}
κ_{I}	phytoplankton growth, light dependence	10 Wm^{-2}
k_{N}	phytoplankton growth, nutrient dependence	0.1 μmol/kg
μ_{P}	phytoplankton metabolism	0.03 day^{-1}
w_{P}	sinking velocity for phytoplankton	1 m/day
γ_{Z}	zooplankton growth rate	1.1 (μmol/kg day)$^{-1}$
κ_{P}	half-saturation constant for zooplankton feeding on phytoplankton	1.5 μmol/kg
ε_{Z}	description of zooplankton sloppy feeding	0.2
$^1\mu_{\text{Z}}$	linear zooplankton metabolism	0.05 day^{-1}
$^2\mu_{\text{Z}}$	quadratic zooplankton metabolism	0.15 (μmol/kg day)$^{-1}$
μ_{D}	bacterial degradation of detritus	0.3 day^{-1}
w_{D}	sinking velocity for detritus	10 m/day
S^{u}	parameter that describes the flux of zooplankton between deep water and surface water	0.67 μmol m/kg day
S^{d}	parameter that describes the flux of zooplankton between deep water and surface water	2 μmol m/kg day

dependence, $I_{\lim}(I)$, governed by the parameter κ_I, the nutrient concentration according to the Michaelis-Menton function and, finally, it is proportional to P. M_P, the metabolism for phytoplankton describes the metabolic cost and natural death, it includes a rate constant μ_P and is proportional to $g(T)$ and P. Values of the constants are given in Table 2 and are taken from Eppley (1972), Sakshaug and Slagstad (1991) and Broström (1997).

2.3.4. Details of zooplankton equation. G_Z, the growth of zooplankton includes a rate constant, γ_Z, a temperature dependence $g(T)$, the phytoplankton concentration according to a Holling type II equation (Steele and Henderson, 1992) and the zooplankton concentration Z. The egestion term for zooplankton, E_Z, includes inefficiency of eating and the production of fecal pellets by zooplankton. We assume that the egestion is proportional to G_Z.

The zooplankton metabolism, M_Z, involves a temperature dependence, $g(T)$, and a "rate constant" $({}^1\mu_Z + {}^2\mu_Z Z)$. The first term describes direct metabolic cost for zooplankton and the second term represent losses connected to internal grazing within the zooplankton community (Steele and Henderson, 1992). The values of the constants γ_Z, κ_P, ε_Z and ${}^2\mu_Z$ are strongly related to the phytoplankton, zooplankton and nitrate concentrations in spring and early summer (Broström, 1997). Thus, the parameters have been set to values that allow the model to reproduce these quantities.

2.4. DOC model

The purpose of this section is to build a model that describes buildup and degradation of DOC that are compatible with data and the present knowledge of the DOC/microbial loop (Taylor and Joint, 1990). We start by giving a short review of some important aspects of the DOC dynamics, e.g., its residual time scale and concentration in sea water.

The strategies we use to build the model are: (1) select the variables needed to describe the basic properties of the DOC cycle; (2) find a model structure and parameter setup that allow the model to reproduce data from station M. We use a simple model formulation to describe the DOC dynamics. The model is, however, built on a more basic model structure for the microbial loop (*Appendix A*).

2.4.1. General description of DOC. DOC may be classified into at least two different categories with respect to its residual timescales (Amon and Benner, 1994; Carlson et al., 1994; Guo et al., 1995; Hansell et al., 1995). One portion is highly stable and has a residual timescale of approximately 4000 years and its concentration is about 50–60 μmol/kg. Deep water contains mainly this form of DOC.

The other pool is more labile, it corresponds to 20–30 μmol/kg and is mainly found in the upper ocean. The residual timescale of the labile pool is more uncertain and estimates range between days/months to decades. The labile pool may also be divided into several categories with different characteristic residual timescales. The concentration of the labile pool may be important for the upper ocean carbon cycle on an annual basis and it is included in the model as ΔDOC.

Kirchman et al. (1991) made some experiments to study the turnover time of DOC. They showed that parts of the DOC may have decay rates as high as 0.25–0.36 day^{-1} during the first day of incubation although most values were about 0.05 day^{-1}. Amon and Benner (1994) studied low- and high-molecular-weight material and concluded that the former had a turnover time of 26 days whereas the latter turned over in 6 days. Hansell et al. (1995) measured an increase in C_T corresponding to a timescale of approximately 10 days for the labile DOC pool.

2.4.2. ΔDOC model. Let us write the model for ΔDOC as,

$$\mathcal{F}(\Delta\text{DOC}) = P_{\Delta\text{DOC}} - M_{\Delta\text{DOC}}, \tag{14}$$

where $P_{\Delta\text{DOC}}$ is the production of labile DOC, determined by the production of phytoplankton. $M_{\Delta\text{DOC}}$ is the bacterial degradation of labile DOC and depends on: (1) the bacterial growth rate; (2) the extent to which bacteria can utilize labile DOC; (3) the size of the bacterial population.

The fluxes in eq. (14) are described by,

$$P_{\Delta\text{DOC}} = \phi G_P \frac{x}{y},$$

$$M_{\Delta\text{DOC}} = \mu_{\Delta\text{DOC}} \frac{\Delta\text{DOC}}{\kappa_{\Delta\text{DOC}} + \Delta\text{DOC}}, \tag{15a, b}$$

where ϕ is the fraction of ΔDOC that is produced for each mol of organic carbon that is produced, $\mu_{\Delta DOC}$ is the rate of the bacterial degradation of ΔDOC and $\kappa_{\Delta DOC}$ is the half saturation constant for bacterial consumption of ΔDOC (see *Appendix A*).

The flux of nutrients, F, involved in the DOC model is given by,

$$F = -\frac{y_{DOC}}{x_{DOC}}(P_{DOC} - M_{DOC}), \quad (16)$$

where $x_{DOC}:y_{DOC}$ is the C:N ratio for DOC. We use $x_{DOC}:y_{DOC}=15$.

2.4.3. Analyzing the ΔDOC equation. Although we have fair knowledge of the microbial loop, it does not necessarily mean that we reproduce measurements from station M. Since we introduce the DOC dynamics and the microbial loop to reduce some uncertainties in the carbon cycle, it is necessary to reproduce measurements for a further comparison.

Let us first consider the production of DOC. Taylor and Joint (1990) used $\phi=0.1$ to link the production of DOC to the production of organic material, however, they also prescribed that a certain amount of, e.g., zooplankton grazing, contributes to the DOC production. Myklestad et al. (1989) stated that under rapid growth conditions about 5–10% of the total photosynthetic carbon production is released as extracellur material whereas it can be as high as 60% under nutrient depletion. The portion released as extracellur material can change considerably between species and depend on light and nutrient conditions with values as high as 50–100%. However, the most common values are in the range 3–10% (Sakshaug, 1993 and references therein). Sloppy feeding by zooplankton is also a source of ΔDOC although an estimate of its importance is difficult to obtain. To describe both processes we assume that 0.15 mol of ΔDOC is produced for each mol of planktonic organic carbon that is produced, thus, we use $\phi=0.15$.

Running the model without the ΔDOC consumption we end up with a maximum ΔDOC value of 45 μmol/kg about 100 days after the start of the spring bloom. Observations according to Børsheim and Myklestad (1997) show that the maximum value is about 20 μmol/kg, implying that there should be a bacterial degradation of approximately 0.25 μmol/(kg day). Thus, if $\Delta DOC \gg \kappa_{\Delta DOC}$ we have that,

$\mu_{\Delta DOC}=0.25$ μmol/(kg day).

According to *Appendix A*, $\mu_{\Delta DOC}$ is related to the potential bacterial consumption of ΔDOC times the bacteria concentration. If the microbial loop is in an quasi-steady state, the bacteria concentration can be related to the parameters of the zooplankton equation. We have,

$$\mu_{\Delta DOC}=\gamma_B\left[\frac{\mu_{mz}}{(1-\varepsilon_{mz})\gamma_{mz}} - p_s\right], \quad (17)$$

where γ_B is the bacterial growth rate, γ_{mz} is the growth rate for microzooplankton, ε_{mz} is the egestion for microzooplankton, μ_{mz} is the metabolism for microzooplankton and p_S is a prescribed picoplankton concentration.

If we solve eq. (17) for p_S and insert the values in Table 3, we have that $p_S \approx 0.4$ μmol C/kg. If we compare the strength of $\mu_{\Delta DOC}$ with and without the picoplankton we see that the bacterial consumption of DOC is reduced by 80% if we allow a picoplankton concentration of the size suggested above. This number is highly sensitive to the values of the constants involved and should be viewed with some caution. Nevertheless, we conclude that the picoplankton may affect the DOC dynamics.

2.5. Chemical model

2.5.1. Basic assumptions. The basic assumption in the chemical model is that the carbon system follows changes in the biological system according to a C:N ratio for biological material. The carbon cycle is related to organic material as,

$$xCO_2 + yNO_3^- + zH_3PO_4 + yH^+ + (x+y)H_2O \Leftrightarrow (CH_2)_x(NH_3)_y(H_3PO_4)_z + (x+2y)O_2, \quad (18)$$

where $(x:y:z)=(106:16:1)$ for N, P, Z_{tot} and D, for ΔDOC we use $(x:y:z)=(240:16:1)$.

The partial pressure of CO_2 in water, pCO_2^W, is calculated from T, S, C_T and A_T (UNESCO, 1987; Peng et al., 1987). However, the C_T data from the TTO/NAS cruise were calculated from alkalinity and pCO_2^W measurements. To have our chemical model consistently with these measurements we use the same constants in our routine to calculate pCO_2^W as was used by Brewer et al. (1986).

2.5.2. Basic equations. With the nutrient flow structure described in eqs. (9) and the DOC cycle in eq. (14) we have,

$$\mathscr{F}(C_T) = -\frac{x}{y}(G_P - M_P - M_Z - M_D) - (P_{DOC} - M_{DOC}),$$

$$\mathscr{F}(A_T) = G_P - M_P - M_Z - M_D. \qquad (19a, b)$$

2.5.3. Boundary conditions. The boundary conditions for C_T and A_T are given by flux conditions,

$$v_t\left(\frac{\partial C_T}{\partial z}, \frac{\partial A_T}{\partial z}\right) = \begin{cases}(Q_{C_T}, 0) & \text{at } z = 0,\\ (0, 0) & \text{at } z = -H,\end{cases} \qquad (20a–d)$$

where Q_{C_T} is the flux of CO_2 at the sea surface. We consider variables normalized to 35 psu, implying that we can neglect the influence of the freshwater flux on the chemical variables.

According to Liss and Merlivat (1986) the flux of CO_2 may be written as,

$$Q_{C_T} = k_{W\text{-}CO_2}\alpha_{CO_2}(pCO_2^W - pCO_2^A), \qquad (21)$$

where $k_{W\text{-}CO_2}$ is the transfer velocity for CO_2, α_{CO_2} is the gas solubility for CO_2 and pCO_2^A is the partial pressure of CO_2 in the atmosphere. A formula for pCO_2^A at station M is obtained by a harmonic fit,

$$pCO_2^A(t) = 336.2 + 1.6t' + 0.72\cos(2\pi t') + 6.1\sin(2\pi t') + 0.98\cos(4\pi t') - 1.7\sin(4\pi t'), \qquad (22)$$

where $t' = t - 1979$, given in years and pCO_2^A is given in ppm of atmospheric pressure (Drange, 1994).

$k_{W\text{-}CO_2}$ may be described in terms of the wind speed at 10 m height, W_{10}, and the Schmidt number for CO_2, Sc_{CO_2} (the ratio of molecular viscosity to molecular diffusivity for CO_2). Wanninkhof (1992) proposed the function,

$$k_{W\text{-}CO_2} = 0.31\left(\frac{660}{Sc_{CO_2}}\right)^{1/2} W_{10}^2, \qquad (23)$$

where $k_{W\text{-}CO_2}$ is given in cm/h. It should be noted that other estimates of the exchange coefficient (Liss and Merlivat, 1986; Woolf and Thorpe, 1991) have different Sc dependencies for low wind speeds and are $\sim 30\%$ weaker at high wind speeds.

To calculate Sc_{CO_2}, we use the temperature dependent viscosity from CRC Handbook of Chemistry and Physics 1983–1984 and the temperature dependent diffusion coefficients for CO_2 by Holmén and Liss (1984). The solubility of CO_2 is taken from Weiss (1974).

2.5.4. Initial conditions. The initial conditions are given by: $C_T = 2120$ μmol/kg in the upper 200 m and decreases linearly from 2145 μmol/kg at 200 m to 2125 μmol/kg at 500 m. $A_T = 2310$ μmol/kg for all depths. These numbers are taken from measurements before the production starts.

3. Model results and comparison with measurements

3.1. Station M

The model is run for the year 1991 and the resulting N, ΔDOC and C_T at 10 m depth together with measurement are shown in Fig. 2. The modeled N describes the observed NO_3 very well on the annual basis (Fig. 2a). However, considering that there is some ammonium in summer, it is possible that the model underestimates N in summer.

The ΔDOC agrees well with the measurements recalculated from Børsheim and Myklestad (1997) (Fig. 2b), especially when taking into account that the DOC concentration usually is higher at the 2–10 m depth as compared with the 25–50 m depth (Børsheim and Myklestad, 1997). In 1992, the DOC concentrations are much higher than the other years implying that our interpretation of ΔDOC may be uncertain. Neglecting the measurements from 1992, the model, possibly, underestimates the ΔDOC in the autumn.

The C_T is shown in Fig. 2c and the inclusion of DOC in the model improves the model-measurement comparison although the model still produces too high values of C_T. The remaining deviation may be the result of: (1) a faulty ΔDOC dynamics; (2) an erroneous in the C : N ratio for organic material; (3) an incorrect description of air–sea flux of CO_2.

The formulation of the air-sea gas exchange is one of the major uncertainties in the model and the formulation according to Wanninkhof (1992) is at the higher end of the gas exchange coefficients

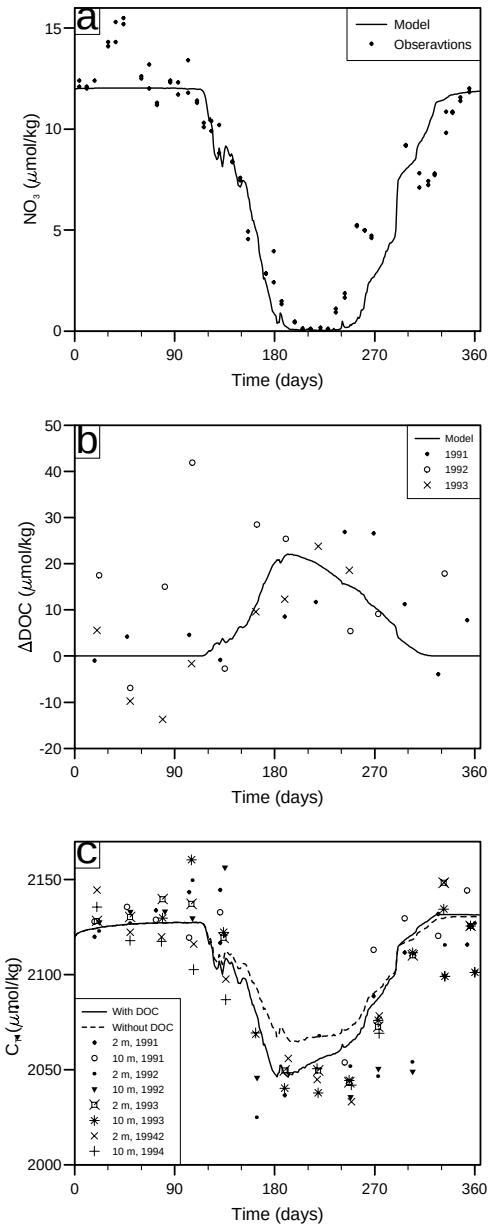

Fig. 2. Model and observations of (a) NO_3, (b) ΔDOC and (c) C_T at station M. The nitrate observations are obtained from F. Rey (personal communication), the ΔDOC observations are recalculated from measurements presented in Børsheim and Myklestad (1997). We have taken the mean value of observations from depth 2, 10, 25 and 50 m minus the mean of observations at the 100 and 200 m depth. The measurements of C_T are from Gislefoss (1994).

(Liss and Merlivat, 1986; Woolf and Thorpe, 1991). If we use the gas exchange coefficient described by Liss and Merlivat (1986), the model produces results that are close to measurements. The final interpretation is thus sensitive to the choice of formulation for the gas exchange coefficient.

Assuming that the air-sea gas exchange is described correctly we may tune the C : N ratio for organic material to fit measurements. Experiments with a C : N = 9 ratio for organic material decreases the modeled surface C_T by approximately 20 μmol/kg in summer which gives a close agreement with data. However, such detailed interpretation of the data is vulnerable considering the uncertainties in the air-sea gas exchange.

3.2. *Three profiles from TTO/NAS expedition*

There are 3 stations from the TTO/NAS expedition that are relatively close to station M, namely stations 143, 144 and 145 (Fig. 1). The temperature is 3°C lower at the TTO/NAS stations as compared to station M implying that the forcing and initial conditions must be modified if we use data from station M to force the model. By setting $Q_{in} = 0$°C/year, the initial condition 3°C lower and using a 3°C lower air temperature we reproduce the temperature profile at the TTO/NAS stations. The modeled N, ΔDOC and C_T for day 207 on year 1981 are shown in Fig. 3 with measurements from the TTO/NAS expedition.

It is notable that the model underestimates the NO_3 concentration in the upper layer, especially taking into account that the NH_4 concentration may be high in summer. Apart from the low values in the upper layer, the modeled N reproduces the measurements well.

The modeled C_T is, however, again higher than measurements. Further, the concentrations in the thermocline are too high. Accordingly, the turbulent diffusion of C_T from these levels may be too high giving too high concentrations in the mixed layer. The C_T are, however, too high in the upper 100 m which suggests that the main explanation must be sought in the air–sea gas exchange formulation or in the C : N ratio for organic material.

3.3. *Stations in the Nordic seas*

How can we analyze the C : N ratio of biological production from data taken at different locations

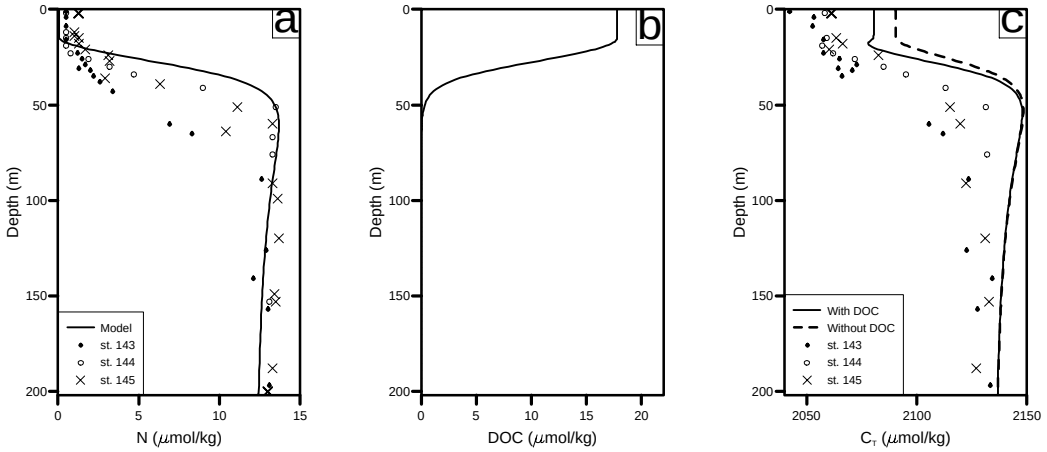

Fig. 3. (a) Modeled and observed NO_3, (b) modeled ΔDOC and (c) modeled and observed C_T. Observations are from the TTO/NAS stations 143–145. The inclusion of ΔDOC in the model significantly improves the model results. The disagreement between model and measurements is within the uncertainty of the description of the air-sea gas exchange of CO_2.

in the Nordic seas? One possibility is to run the model for each location and interpret data locally. However, because of the uncertainties introduced when extracting forcing from atmospheric models, we have abandoned this possibility at the present stage.

Another possibility is to investigate the observed chemical signature, e.g., the property-property plot of depletion of NO_3 versus depletion of C_T, with the signatures of the model. We prefer to work with depletion of nutrient concentrations and C_T to remove the spatial variability. The depletion, denoted with Δ, is defined differently for measurements and model. For measurements it is defined as the difference between the observed value minus the mean value of the measurements between 100–400 m depth. This calculation is performed for each individual station. For the model, Δ is defined as the modeled value minus the value at 200 m depth (the figures show the modeled values for the upper 100 m). The model values are derived from the profiles in Fig. 3a and some additional experiments. Note that we treat the model variable N as NO_3 which is somewhat incorrect since there may be some ammonium present as well. Furthermore, to avoid the low salinity water from the Greenland current that have a different water composition (Takahashi et al. 1985) we only use measurements with salinity greater than 34 psu.

Fig. 4a show ΔNO_3 versus ΔC_T for the measurements taken at the TTO/NAS expedition together with model results. Observe that the modeled depletion of C_T is too small below the 30 m level. The case without the air-sea exchange shows too strong depletion of C_T showing that the final interpretation of data depends on the strength of the air-sea gas exchange.

To check that the production of $CaCO_3$ from shell building organisms can be neglected, we show ΔA_T versus ΔNO_3 in Fig. 4b. There are no major deviations between the model and measurements. The good agreement between data and model shows that the Greenland current water, which has a different A_T and C_T signature, has not influenced the surface water in an important way. Thus, we may conclude that the low salinity that appears at some of the TTO/NAS stations probably are the result of melting ice.

Figure 4c shows ΔC_T versus ΔPO_4 for the Mosby cruise from 1991. ΔPO_4 for the model is defined from ΔNO_3 according to the Redfield ratio. The scatters in the measurements from the Mosby cruise are significantly higher than the measurements from the TTO/NAS expedition but the pattern is similar to that in Fig. (4 a).

The modeled deviations from the Redfield ratio in Figs. 4a, c are due to, (1) production of ΔDOC and (2) air-sea gas exchange of CO_2. The present model configuration indicates that the gas exchange is somewhat stronger than the consumption of C_T from DOC production. However, the

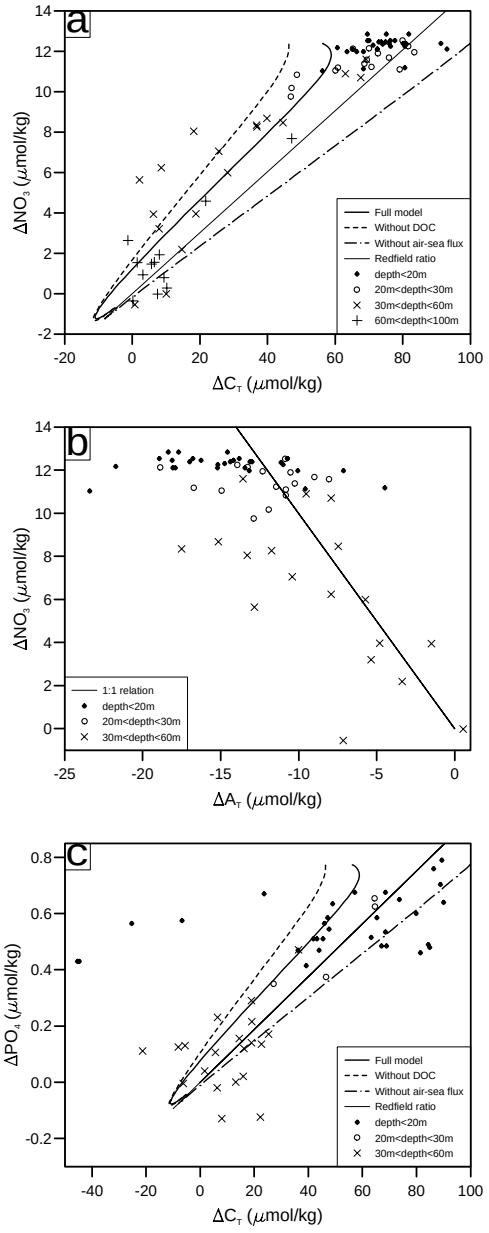

Fig. 4. (a) The normalized ΔC_T versus ΔNO_3 for the TTO/NAS expedition, (b) the normalized ΔA_T versus ΔNO_3 for the TTO/NAS expedition and (c) the normalized ΔC_T versus ΔPO_4 for the Mosby cruise. See the text for details about the procedure to obtain ΔC_T, ΔNO_3 and ΔPO_4. The model data are taken from Fig. 3. The thin line is the Redfield ratio and the thicker line corresponds to modeled C_T values. The dashed line is the model with $\Delta DOC = 0$ and the dashed dotted line is the model with the air-sea exchange shut off. Phosphate measurements have been used from the Mosby cruise as there were only few nitrate measurements.

processes are of similar strength and the production seemingly follows the Redfield ratio making it easy to misinterpretate data.

4. Results and discussion

In this study, we investigate the biological consumption of total dissolved inorganic carbonate concentration versus consumption of nitrate and phosphate concentrations in the Nordic seas. Børsheim and Myklestad (1997) showed that the DOC concentration may change significantly on both seasonal and annual timescales at station M. We conclude that DOC with a high carbon content must be included into models of the carbon cycle to explain the draw-down of C_T in summer.

The main tool that we use to interpret data is a physical-biological-chemical model that is described in Section 2. Furthermore, in Appendix A, we discuss a simple model for the labile DOC concentration based on a model for the DOC cycle and the microbial loop (Taylor and Joint, 1990).

An important feature of the DOC model is that microzooplankton can graze on picoplankton. The presence of picoplankton implies that the microzooplankton can become abundant enough to significantly reduce the bacterial concentration. The picoplankton concentration, denoted as p_S, was calculated from the requirement that the model should reproduce measurements of ΔDOC. From the calculation we obtain, $p_S \approx 0.4$ μmol C/kg and an associated 80% reduction of the bacterial consumption of labile DOC. The labile DOC concentration for different values of the stipulated p_S concentration is shown in Fig. 5. The case with $p_S = 0.5$ μmol C/kg represent the situation when bacterial consumption of labile DOC is zero and the case with $p_S = 0$ μmol C/kg describes the bacterial degradation of labile DOC if microzooplankton can only use bacteria as a food source. Obviously, the possibility that microzooplankton has an additional food source is very important for the modeled ΔDOC, possibly explaining the high DOC concentrations that are

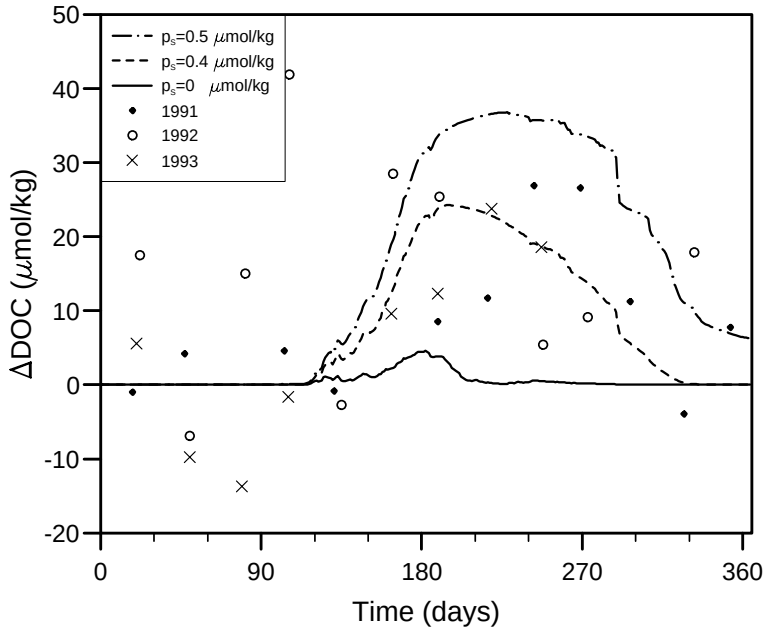

Fig. 5. The modeled ΔDOC for different values of the stipulated picoplankton concentration, p_S. We see that the presence of picoplankton can have a dramatic influence on the labile DOC concentration.

found in the summer mixed layer at station M. However, the fraction, ϕ, of the phytoplankton production that is released as DOC, is also an important parameter in the ΔDOC model. Although not shown, the levels of the ΔDOC in Fig. 5 depend almost linearly on the value of ϕ.

The inclusion of DOC in the carbon cycle improves the comparison between the modeled C_T and measurements. However, there are some indications, although not conclusive, that there is an additional draw-down of the C_T that we cannot account for. Possibly, it may be export of particles with high carbon content that is the result of (1) selective mineralization or (2) the production of organic material with high C : N ratio.

Assuming that the gas exchange formulation is correct (Wanninkhof, 1992) we may perform some experiments with different C : N ratios for organic material (Fig. 6). Notably, the experiment with the C : N = 9 ratio is closest to measurements. However, there are great uncertainties in the formulation of the gas exchange coefficient hampering the comparison between data and model. With the gas exchange coefficient described by Liss and Merlivat (1986) no such conclusions on the C : N ratio for organic material can be drawn. Albeit that, a C : N ratio of 9 is commonly found in the material caught by sediment traps in the North Atlantic confirming our interpretation of data (Honjo, 1980; Bathmann et al., 1991; Buesseler et al., 1992; Honjo and Manganini, 1993). Further, data from the TTO/NAS expedition shows that the thermocline water in the "Gulf Stream" part of the North Atlantic have a ΔC : ΔN = 9 ratio (Broström, 1997).

It is notable that the ΔDOC in the model decays faster than measurements suggest. Possibly, ΔDOC should be described by two different categories with different production and consumption rates. In this study of the upper layer and on a seasonal timescale the present model works satisfactorily (we are mainly interested in the accumulation of labile DOC during the summer). However, if we turn the interest to the annual dynamics and the possibility that labile DOC may be exported to the deep water with the winter convection, a more detailed description of the different ΔDOC pools should be introduced.

It has been suggested that the buildup of DOC in the upper waters during summer can lead to a

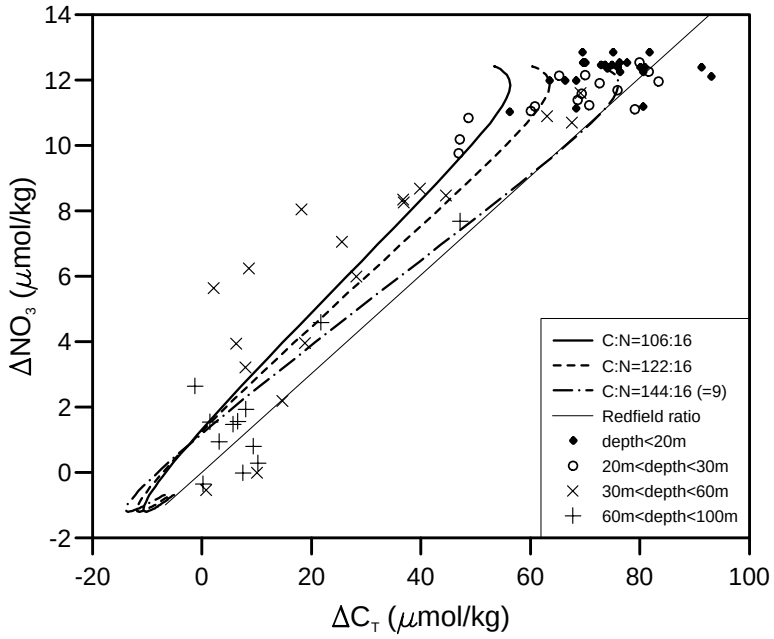

Fig. 6. The modeled draw-down of C_T relative NO_3 for different values of the C : N ratio for organic material.

strong transport of organic carbon to deeper waters during the winter convection (Christensen et al., 1989; Copin-Montégut and Avril, 1993; Carlson et al., 1994; Chen et al., 1996). However, if the convection is not deep enough, say more than 300 m, the DOC influence is trapped in the near-surface region that is in contact with the atmosphere. Of course, there can be some downward diffusion of labile DOC but, probably, it can never significantly influence the carbon budget below, say 500 m. In areas of deep water convection (e.g., the Nordic seas, parts of the Mediterranean and around the Antarctic) the summer production of labile DOC may have a strong influence on the deep water concentration of DOC (Christensen et al., 1989; Copin-Montégut and Avril, 1993). With the mineralization of labile DOC the bottom water total dissolved inorganic carbonate concentration will inevitably be influenced and by that the global carbon budget.

The chemical composition of deep water suggests that mineralization of organic material deviates from the Redfield ratio (Takahashi et al., 1985; Christensen et al., 1989) although the deviation is not as large as it is in the upper water column (Sambrotto et al., 1993; Michaels et al., 1994). Thus, the processes responsible for the non-Redfield behavior in the upper ocean do not fully penetrate into the deeper layers. Possibly, DOC production may be important in the upper ocean but it is only important for the deep-water C_T in regions with deep water formation. How mineralization of labile DOC will influence the C : N : P ratios of deep waters is, however, not yet clarified.

5. Acknowledgment

I would like to thank Professor Gösta Walin for many discussions on the formulation of the model and interpretation of data. Fransisco Rey at the Marine Research Institute in Bergen, Norway, provided the unpublished data of nitrate concentration for station M. Two anonymous reviewers gave valuable comments on an early draft of this manuscript. The work is a part of a Scandinavian work group that investigates the flux of carbon dioxide in the Nordic seas and is sponsored by the Nordic Council of Ministers.

Appendix A

In this appendix, we attempt to discuss some properties of the bacterial consumption of dissolved organic carbon, DOC. The main point

is to highlight the importance of picoplankton on the bacteria abundance.

The DOC and microbial loop model include the labile DOC concentration, ΔDOC, bacteria, B, picoplankton, p, and microzooplankton, mz. Bacteria utilize ΔDOC and the microzooplankton consume bacteria and picoplankton. We include picoplankton in the model as it is an important food source for the microzooplankton population. The microzooplankton population is very important for the bacteria population which in turn use the DOC. We do not consider a coupling of the microzooplankton to the zooplankton in the biological model, Subsection 2.3, although there certainly is such a coupling. However, the model behavior for DOC is not particularly sensitive to the exact model formulation in this case.

Let us write the following equation for the change in ΔDOC,

$$\mathcal{F}(\Delta\mathrm{DOC}) = \phi G_{\mathrm{P}} \frac{x}{y} - \gamma_{\mathrm{B}} \frac{\Delta\mathrm{DOC}}{\kappa_{\Delta\mathrm{DOC}} + \Delta\mathrm{DOC}} B, \tag{A1}$$

where ϕ is the fraction of ΔDOC produced for each mol of organic carbon that is produced, G_{P} is the production of phytoplankton in nitrogen units, $x:y = 106:16$ represents the carbon to nitrogen content of the phytoplankton, γ_{B} is the rate at which bacteria can utilize ΔDOC, κ_{DOC} is the half saturation constant for bacterial utilization of ΔDOC. Thus, to describe the bacterial breakdown of ΔDOC we must find the bacterial concentration. The bacteria concentration can be found from the equation that describes the microzooplankton population,

$$\mathcal{F}(\mathrm{mz}) = (1-\varepsilon_{\mathrm{mz}})\gamma_{\mathrm{mz}}(B+\mathrm{p})\mathrm{mz} - \mu_{\mathrm{mz}}\mathrm{mz}, \tag{A2}$$

where γ_{mz} is the microzooplankton grazing rate, $\varepsilon_{\mathrm{mz}}$ reflects the microzooplankton egestion, we assume that the grazing rate is proportional to both bacteria and picoplankton, finally, μ_{mz} is the metabolic and grazing losses from the microzooplankton population.

We may assume that the microbial loop is in a quasi-stationary state during the productive season (Taylor and Joint, 1990), i.e., a state where one or more of the time derivatives in the model equations have lost their influence. An example is provided by the early summer after the initial part of the spring bloom. During this phase the biological model presented in Subsection 2.3 has fairly constant phyto- and zooplankton concentrations while the nitrate concentration decreases monotonously. In the quasi-steady state, the phyto- and zooplankton concentrations are set by internal relations in the equations and are unaffected by the history.

If the biological model is in a quasi-steady state it is reasonable to assume that the microbial loop is in a quasi-steady state as well. To find how the abundance of picoplankton may influence the predicted bacterial concentration we consider the picoplankton concentration as an externally described parameter with concentration p_{S}. Accordingly we drop the time derivative in eqs. (A2) and put $p = p_{\mathrm{S}}$. Then solving the equation for B,

$$B = \frac{\mu_{\mathrm{mz}}}{(1-\varepsilon_{\mathrm{mz}})\gamma_{\mathrm{mz}}} - p_{\mathrm{s}}. \tag{A3}$$

Obviously, B is very critical to the stipulated picoplankton concentration. The possibility to graze on picoplankton can make the zooplankton abundant enough to reduce the bacterial pool. With low bacterial concentrations, the consumption of DOC will be small allowing a buildup of DOC in the water.

If B is known according to eq. (A3), we also know the bacterial consumption of DOC whereby the model for DOC is complete.

Table 3. *Constants in the DOC and microbial loop model*

Constant	Meaning	Value
ϕ	fraction of DOC produced for each unit of organic C that is produced	0.15
$\mu_{\Delta\mathrm{DOC}}$	bacterial degradation of DOC	0.25 μmol/kg day
γ_{B}	growth rate for bacteria	2 day^{-1}
k_{DOC}	half-saturation constant for bacteria growth on DOC	1 μmol/kg
γ_{mz}	microzooplankton growth rate	2 day^{-1}
$\varepsilon_{\mathrm{mz}}$	efficiency of microzooplankton feeding on bacteria and picoplankton	0.5
μ_{mz}	microzooplankton metabolism and grazing	0.5 day^{-1}

REFERENCES

Amon, R. M. W. and Benner, R. 1994. Rapid cycling of high-molecular-weight dissolved organic matter in the ocean. *Nature* **369**, 549–552.

Anderson, L. A. 1995. On the hydrogen and oxygen content of marine phytoplankton. *Deep-Sea Res.* **42**, 1675–1680.

Anderson, L. A. and Sarmiento, J. L. 1994. Redfield ratios of remineralization determined by nutrient data analysis, *Global Biogeochem. Cycles* **8**, 65–80.

Bates, N. R., Michaels A. F. and Knap, A. H. 1996. Seasonal and interannual variability of oceanic carbon dioxide species at the U. S. JGOFS Bermuda Atlantic Time-series Study (BATS) site. *Deep-Sea Res. II* **43**, 347–384.

Bathmann, U. V., Noji, T. T. and von Bodungen, B. 1990. Copepod grazing potential in late winter in the Norwegian Sea — a factor in the control of spring phytoplankton growth? *Mar. Ecol. Prog. Ser.* **60**, 225–233.

Bathmann, U. V., Noji, T. T. and von Bodungen, B. 1991. Sedimentation of pteropods in the Norwegian Sea in autumn. *Deep-Sea Res.* **38**, 1341–1360.

Børsheim, K. Y. and Myklestad, S. M. 1997. Dynamics of DOC in the Norwegian Sea inferred from monthly profiles collected during three years at 66°N 2°E. *Deep-Sea Res.* **44**, 593–601.

Brewer, P. G., Takahashi, T. and William's, R. T. 1986. Transient Tracers in the ocean (TTO) — Hydrographic data and carbon dioxide systems with revised carbon chemistry data, *NDP-004/R1*. Carbon Dioxide Information Analysis Center (CDIAC), Oak Ridge National Laboratory, Oak Ridge, Tennessee, USA.

Broström, G. 1997. *Interaction between mixed layer dynamics, gas exchange and biological production in the oceanic surface layer with application to the northern North Atlantic*. PhD thesis. Department of Oceanography, Göteborg University, Gothenburg, Sweden.

Buesseler, K. O., Bacon, M. P., Cochran, J. K. and Livingstone, H. D. 1992. Carbon and nitrogen export during the JGOFS North Atlantic Bloom Experiment estimated from $^{234}Th:^{238}U$ disequilibium. *Deep-Sea Res. II* **39**, 115–117.

Carlson, C. A., Ducklow, H. W. and Michaels, A. F. 1994. Annual flux of dissolved organic carbon from the euphotic zone in the northwestern Sargasso Sea. *Nature* **371**, 405–408.

Chen, F. R., Fry, B., Hopkinson, C. S., Repeta, D. J. and Peltzer, E. T. 1996. Dissolved organic carbon on Georges Bank. *Cont. Shelf Res.* **16**, 409–420.

Christensen, J. P., Packard, T. T., Dortch, F. Q., Minas, H. J., Gascard, J. C., Richez, C. and Garfield, P. C. 1989. Carbon oxidation in the deep Mediterranean sea: evidence for dissolved organic carbon source. *Glob. Biogeochem. Cycles* **3**, 315–335.

Codispoti, L. A., Friederich, G. E., Iverson, R. I. and Hood, D. W. 1982. Temporal changes in the inorganic carbon system of the south-eastern Bering Sea during spring 1980. *Nature* **296**, 242–245.

Codispoti, L. A., Friederich, G. E. and Hood, D. W. 1986. Variability in the inorganic carbon system over the southeastern Bering Sea shelf during spring 1980 and spring-summer 1981. *Cont. Shelf Res.* **5**, 133–160.

Copin-Montégut, G. and Avril, B. 1993. Vertical distribution and temporal variation of dissolved organic carbon in the North-Western Mediterranean Sea. *Deep-Sea Res.* **40** 1963–1972.

Drange, H. 1994. *An isopycnic coordinate carbon cycle model for the North Atlantic; and the possibility of disposing of fossil fuel CO_2 in the ocean.* PhD thesis. Nansen Environmental and Remote Sensing Centre, Bergen, Norway.

Eppley, R. W. 1972. Temperature and phytoplankton growth in the sea. *Fish. Bull.* **70**, 1063–1085.

Follows, M. J., Williams, R. G. and Marshall, J. C. 1996. The solubility pump of carbon in the subtropical gyre of the North Atlantic. *J. Mar. Res.* **54,** 605–630.

Gargett, A. E. 1984, Vertical eddy diffusivity in the ocean interior. *J. Mar. Res.* **42**, 359–393.

Gislefoss, J. S. 1994. *Carbon profiles in the Nordic seas.* PhD thesis, Radiological Dating Laboratory, Faculty of Physics and Mathematics, Norwegian Institute of Technology, Trondheim, Norway.

Guo, L., Santschi, P. H. and Warnken, K. 1995. Dynamics of dissolved organic carbon (DOC) in oceanic environments. *Limn. Oceanogr.* **40**, 1392–1403.

Häkkinen, S. and Cavalieri, D. J. 1989. A study of oceanic surface heat fluxes in the Greenland, Norwegian and Barents Seas. *J. Geophys. Res.* **94**, 6145–6157.

Hansell, D. A., Bates, N. R. and Gundersen, K. 1995. Mineralization of dissolved organic carbon in the Sargasso Sea. *Mar. Chem.* **51**, 201–212.

Holmén, K. and Liss, P. 1984. Models for air-water gas transfer: an experimental investigation. *Tellus* **36B**, 92–100.

Honjo, S. 1980. Material fluxes and modes of sedimentation in the mesopelagic and bathypelagic zones. *J. Mar. Res.* **38**, 53–97.

Honjo, S. and Manganini, S. J. 1993. Annual biogenic particle fluxes to the interior of the North Atlantic Ocean; studied at 34°N 21°W and 48°N 21°W. *Deep-Sea Res.* **40**, 587–607.

Kirchman, D. L., Suzuki, Y., Garside, C. and Ducklow, H. W. 1991. High turnover rates of dissolved organic carbon during spring a phytoplankton bloom. *Nature*, **352**, 612–614.

Large, W. G. and Pond, S. 1981. Open ocean momentum flux measurements in moderate to strong winds. *J. Phys. Oceanogr.* **11**, 324–336.

Liss, P. S. and Merlivat, L. 1986. Air-sea exchange rates: Introduction and synthesis. In: The rôle of air-sea exchange in geochemical cycling, edited by P. Buat-Ménard. *NATO ASI Series, Serie C: Mathematical and*

Physical sciences, **185**, 113–127. D. Riedel Publishing Company, The Netherlands.

Lundberg, L., Molander, S. and Østerhus, S. 1995. *Observations of the carbonate system together with CTD data from cruise with r/v Håkon Mosby in the Norwegian, Greenland and Iceland seas during late summer 1991*. Report 72, Geophysical Institute, Oceanography, Bergen, Norway, 73 pp.

Marchal, O., Monfray, P. and Bates, N. 1996. Spring-summer imbalance of dissolved inorganic carbon in the mixed layer of the Northwestern Sargasso Sea. *Tellus* **48B**, 115–134.

Menzel, D. W. and Ryther, J. H. 1960. The annual cycle of primary production in the Sargasso Sea of Bermuda. *Deep-Sea Res.* **6**, 351–367.

Michaels, A. F., Bates, N. R., Buesseler, K. O., Carlson, C. A. and Knap, A. H. 1994. Carbon-cycle imbalances in the Sargasso Sea. *Nature* **372**, 537–540.

Myklestad, S., Holm-Hansen, O., Vårum, K. M. and Volcani, B. E. 1989. Rate of release of extracellular amino acids and carbohydrates from marine diatom *Chaetoceros affinis*. *J. Plankton Res.* **11**, 763–773.

Østvedt, O.-J., 1955. Zooplankton investigations from weather ship M in the Norwegian Sea, 1948–49. *Hvalrådets Skrifter* **40**, 1–93.

Peng, T.-H., Takahashi, T., Broecker, W. S. and Olafsson, J. 1987. Seasonal variability of carbon dioxide, nutrients and oxygen in the northern North Atlantic surface water: observations and a model. *Tellus* **39B**, 439–458.

Rodi, W. 1980. *Turbulence models and their applications in hydraulics*. International Association Hydraulic Research, Delft, The Netherlands. 104 pp.

Rodi, W. 1987. Examples of calculation methods for flow and mixing in stratified fluids. *J. Geophys. Res.* **92**, 5305–5328.

Sakshaug, E. and Slagstad, D. 1991. Light and productivity of phytoplankton in polar marine ecosystems: a physiological view. *Polar Res.* **10**, 69–85.

Sakshaug, E. 1993. The relationship between phytoplankton growth rate and production with emphasis on respiration and excretion. *ICES Mar. Sci. Symp.* **197**, 63–68.

Sambrotto, R. N., Savidge, G., Robinson, C., Boyd, P., Takahashi, T., Karl, D. M., Langdon, C., Chipman, D., Marra, J. and Codispoti, L. 1993. Elevated consumption of carbon relative to nitrogen in the surface ocean. *Nature* **363**, 248–250.

Sambrotto, R. N. and Langdon, C. 1994. Water column dynamics of dissolved inorganic carbon (DIC), nitrogen and O_2 on Georges bank during April, 1990. *Cont. Shelf Res.* **14**, 765–789.

Sathyendranath, S. and Platt, T. 1988. The spectral irradiance field at the surface and in the interior of the ocean: a model for applications in oceanography and remote sensing. *J. Geophys. Res.* **93**, 9270–9280.

Steele, J. H. and Henderson, E. W. 1992. The role of predation in plankton models. *J. Plankton Res.* **14**, 157–172.

Svensson, U. 1986. PROBE- An instruction manual. *Report Oceanography* **10**, 90 pp., The Swedish Meteorological and Hydrological Institute (SMHI), S-601 76 Norrköping, Sweden.

Takahashi, T., Broecker, W. S. and Langer, S. 1985. Redfield ratio based on chemical data from isopycnal surfaces. *J. Geophys. Res.* **90**, 6907–6924.

Takahashi, T., Olafsson, J., Broecker, W. S., Goddard, J., Chipman D. W. and White, J. 1985. Seasonal variability of the carbon-nutrient chemistry in the ocean areas west and north of Iceland. *Rit Fiskideildar* **9**, 20–36.

Takahashi, T., Olafsson, J., Goddard, J. G., Chipman, D. W. and Sutherland, S. C. 1993. Seasonal variation of CO_2 and nutrients in the high latitude surface oceans: A comparative study. *Glob. Biogeochem. Cycles* **7**, 843–878.

Taylor, A. H. and Joint, I. 1990. A steady-state analysis of the "microbial loop" in stratified systems. *Mar. Ecol. Prog. Ser.* **59**, 1–17.

Toggweiler, J. R., 1994. Vanishing in Bermuda. *Nature* **372**, 505–506.

UNESCO, 1987. Thermodynamics of the carbon dioxide system in seawater. Report by the carbon dioxide subpanel of the JPOTS. *UNESCO Technical Papers in Marine Science* **51**, 55 p. Division of Marine Sciences, UNESCO, Place de Fontenoy, 75700 Paris, France.

Wanninkhof, R., 1992. Relationship between wind speed and gas exchange over the ocean. *J. Geophys. Res.* **97**, 7373–7382.

Weiss, R. F., 1974. Carbon dioxide in water and seawater: The solubility of a non-ideal gas. *Mar. Chem.* **2**, 203–215.

Woolf, D. K. and Thorpe, S. A. 1991. Bubbles and the air-sea exchange of gases in near-saturation conditions. *J. Mar. Res.* **49**, 435–466.